frontiers in Earth Science

ORIGINAL RESEARCH
published: 20 May 2021
doi: 10.3389/feart.2021.664361

Geochronological Constraint on the Evolution of the Aktyuz Terrane, Kyrgyz North Tianshan, and the Fate of the Taldybulak Levoberezhny Gold Deposit

Wei Xi[1,2,3], Nuo Li[1,2], Xiaohong Xia[4,5]*, Xiaoxiao Ling[6] and Yanshuang Wu[1,2]*

[1] Xinjiang Research Centre for Mineral Resources, Xinjiang Institute of Ecology and Geography, Chinese Academy of Sciences, Urumqi, China, [2] Xinjiang Key Laboratory of Mineral Resources and Digital Geology, Urumqi, China, [3] University of Chinese Academy of Sciences, Beijing, China, [4] Sichuan Geological and Mineral Resources Group Co., Ltd., Chengdu, China, [5] Altynken Limited Liability Company, Zijin Mining Group, Bishkek, Kyrgyzstan, [6] State Key Laboratory of Lithospheric Evolution, Institute of Geology and Geophysics, Chinese Academy of Sciences, Beijing, China

OPEN ACCESS

Edited by:
Xiaohua Deng,
Beijing Institute of Geology for Mineral Resources, China

Reviewed by:
Yin-Hong Wang,
China University of Geosciences, China
Yi Zheng,
Sun Yat-sen University, China

***Correspondence:**
Nuo Li
nuolipku@126.com
Xiaohong Xia
xiaxiaohong55555@163.com

Specialty section:
This article was submitted to Economic Geology, a section of the journal Frontiers in Earth Science

Received: *05 February 2021*
Accepted: *07 April 2021*
Published: *20 May 2021*

Citation:
Xi W, Li N, Xia X, Ling X and Wu Y (2021) Geochronological Constraint on the Evolution of the Aktyuz Terrane, Kyrgyz North Tianshan, and the Fate of the Taldybulak Levoberezhny Gold Deposit. Front. Earth Sci. 9:664361. doi: 10.3389/feart.2021.664361

The Aktyuz Terrane in Kyrgyz North Tianshan is of particular interest due to the occurrence of high and ultrahigh pressure (HP–UHP) rocks and it containing the third largest gold deposit in Kyrgyz North Tianshan, i.e., Taldybulak Levoberezhny (abbreviated to Taldybulak Lev.). To constrain the ages of the host Kemin Complex and its auriferous monzogranite porphyry, detailed zircon U–Pb dating [by laser ablation inductively coupled plasma-mass spectrometry (LA-ICPMS) and secondary ion mass spectroscopy (SIMS)] and Lu–Hf isotopic analyses were carried out. The intensively altered auriferous monzogranite porphyry yielded two weighted mean ages of 444 ± 3 Ma (n = 14, mean squared weighted deviation (MSWD) = 0.49, by LA-ICPMS) and 440 ± 5 Ma (n = 8, MSWD = 0.82, by SIMS) that are indistinguishable within error ranges. Such ages are consistent with a previously reported sulfide Re–Os isochron age of 434 ± 18 Ma, supporting a Silurian porphyry gold mineralization. The granitic gneiss yielded a protolith age of 773 ± 7 Ma (n = 7, MSWD = 0.04) and two metamorphic ages of 514 ± 4 Ma (n = 8, MSWD = 0.09) and 483 ± 3 Ma (n = 11, MSWD = 0.04). Detrital zircons from one fuchsite schist sample yielded highly variable ages from 729 ± 13 Ma to 2,463 ± 30 Ma, with 12 data points weighted at 740 ± 5 Ma (MSWD = 0.95). The metamorphic overgrowth yielded a weighted mean age of 460 ± 4 Ma (n = 4, MSWD = 0.15). Detrital zircons in the migmatitic amphibolite are aged from 788 ± 7 Ma to 3,447 ± 32 Ma, with two major concentrations at 941 ± 7 Ma (n = 13, MSWD = 0.95) and 794 ± 5 Ma (n = 8, MSWD = 0.19). The metamorphic overgrowth yielded an average age of 555 ± 4 Ma (n = 8, MSWD = 0.65). The detrital and xenocryst zircons, and evolved εHf(t) values (−20.9 to −7.8) and old two-stage Hf model ages (1,367–3,159 Ma), revealed the presence of a Precambrian basement that may be dated back to the Archean Eon. The two metamorphic ages may correlate with oceanic subduction and continental collision, respectively.

Keywords: zircon U–Pb age, Lu–Hf isotope, Aktyuz terrane, Kyrgyz North Tianshan, Taldybulak Levoberezhny gold deposit

INTRODUCTION

The Central Asia Orogenic Belt (CAOB; **Figure 1A**) is the biggest accretion-type orogen since the Phanerozoic (Windley et al., 2007; Zhu et al., 2007; Gao et al., 2009b; Xiao et al., 2012, 2013). Its southwestern area, i.e., the Tianshan Orogen in Kazakhstan, Kyrgyzstan, and northwest China, is a composite of Paleozoic island arcs, ophiolites, metamorphic complexes, and Precambrian microcontinental terranes that were wedged together during the early Paleozoic (Kröner et al., 2012). The mechanism of Paleozoic accretion, however, remains poorly constrained (Sengor and Natalin, 1994; Charvet et al., 2007, 2011; Windley et al., 2007; Kröner et al., 2012, 2013). Critical questions, such as the geometry, extent, and source of individual terranes or sutures and also the age and origin of medium- to high-grade metamorphic complexes are still unsolved (Alexeiev et al., 2011; Kröner et al., 2012; Rojas-Agramonte et al., 2013). In this context, the high and ultrahigh-pressure (HP–UHP) metamorphic belt that characterizes ancient subduction zones and sutures is of particular interest due to the important information it can provide for the reconstruction of tectonic evolution (Gao and Klemd, 2003; Klemd et al., 2005; Orozbaev et al., 2007, 2010; Gao et al., 2009a).

The Aktyuz terrane is one of two eclogite and garnet amphibolite occurrences in Kyrgyz North Tianshan (Kröner et al., 2012; Rojas-Agramonte et al., 2013). It is composed of two litho-tectonic assemblages, named the Aktyuz and Kemin Complexes. The former is outcropped in the northern area and is well studied because it contains HP–UHP rocks that can be used as a powerful tool for geodynamic reconstruction (Kröner et al., 2012; Rojas-Agramonte et al., 2013). The latter is in the southern area of the terrane and, by contrast, is poorly studied. Kröner et al. (2012) and Rojas-Agramonte et al. (2014) carried out sensitive high-resolution ion microprobe (SHRIMP) zircon U–Pb studies of granitoid gneiss and paragenesis that precisely constrained their protolith age. Nevertheless, their metamorphic timing remains to be elucidated, preventing the correlation with the metamorphism and exhumation of HP–UHP rocks in this region.

Although it does not contain UHP–HP rocks, the Kemin Complex has a giant gold endowment. The Taldybulak Levoberezhny (abbreviated to Taldybulak Lev. hereafter) deposit is the third largest gold deposit in Kyrgyz North Tianshan, with a reserve of Au 130 t and an average grade of 6.9 g/t (Zhao et al., 2015; Xi et al., 2018). Since its discovery in the 1960s, the genesis of the deposit has been hotly debated. The proposed genesis includes porphyry (Djenchuraeva et al., 2008; Trifonov, 2016), orogeny (Goldfarb et al., 2014; Xue et al., 2014), or multiple mineralization involving both orogeny and porphyry (Zhao et al., 2015, 2017). Recently, Xi et al. (2018) recognized massive sulfide ores that are typical for the volcanogenic massive sulfide (VMS) or sedimentary exhalative (SEDEX) system instead of the above-mentioned porphyry or orogenic deposits. Hence, a comprehensive geochronological study of the host rocks and the ore-causative granitic porphyry is invaluable for an improved understanding of the deposit formation and regional tectonic evolution.

In this article, we report the results obtained from an integrated *in situ* U–Pb and Hf isotope analysis of zircon for an auriferous monzogranite porphyry and metamorphic rocks of the Kemin Complex hosting the Taldybulak Lev. deposit. These data provide a well-constrained temporal framework of regional magmatic and metamorphic events. In combination with the previous work, they also shed light on regional tectonic evolution and ore formation.

GEOLOGICAL BACKGROUND

The CAOB is sandwiched between blocks including the plate of Siberia, Eastern Europe, Tarim, Karakum, and North China (**Figure 1A**). It is composed of an island arc, seamount, ophiolite suite, Precambrian micro-continents, and an accretionary wedge and is attributed to the collision between Siberia and the Tarim–North China Block (Windley et al., 2007; Xiao et al., 2009; Chen et al., 2012). The Tianshan Orogen in Kyrgyzstan in the southwestern part of CAOB has been traditionally grouped into three fault-bounded tectonic zones (**Figure 1B**), from south to north, i.e., South Tianshan, Middle Tianshan, and North Tianshan, with the Atbashi-Inylchek suture and Nikolaev Line as the main boundaries (Seltmann et al., 2011; Kröner et al., 2012). Kyrgyz North Tianshan is characterized by several Precambrian microcontinents (or fragments), ophiolite belts representative of a former oceanic basin (e.g., Djalair-Naiman and Kyrgyz-Terskey), and HP–UHP eclogite facies metamorphic rocks (Windley et al., 2007; Glorie et al., 2010; De Grave et al., 2013). There are abundant Andes-type early Paleozoic magmatic rocks, with the Ordovician granitoids considered as products of subduction and subsequent Silurian granitoid as products of post-collision. The Kyrgyz Middle Tianshan contains Devonian to Pennsylvanian passive margin carbonate and siliciclastic facies rocks. It is considered as the deformed southern margin of the Kazakhstan continent (Alexeiev et al., 2019). On its southwestern margin, there are well-developed continental arcs of Silurian, Devonian, and Pennsylvanian origins (Rojas-Agramonte et al., 2014; Alexeiev et al., 2016). The Kyrgyz South Tianshan is dominated by sedimentary assemblages, followed by minor volcanic, metamorphic, and ophiolitic rocks. They are stacked together by a south-facing thrust in an accretionary and collisional setting in the Late Carboniferous and Permian (Han et al., 2011; Alexeiev et al., 2019).

The Aktyuz terrane in Kyrgyz North Tianshan is considered as part of the North Tianshan microcontinent that rifted from the Tarim craton (Rojas-Agramonte et al., 2014). It is bound by the Late Cambrian–Early Ordovician Dzhalair-Naiman ophiolite-bearing suture in the north, and a Grenvillian-age granitic gneiss in the south (Kröner et al., 2012; Rojas-Agramonte et al., 2014; Alexeiev et al., 2019). In this region, there is an extensively exposed Precambrian metamorphic basement including Aktyuz and Kemin Complex rocks. The Aktyuz Complex in the north has an outcropped length of more than 20 km and a width up to 5 km (Orozbaev et al., 2010). It mainly consists of well-foliated pelitic and granitic gneisses

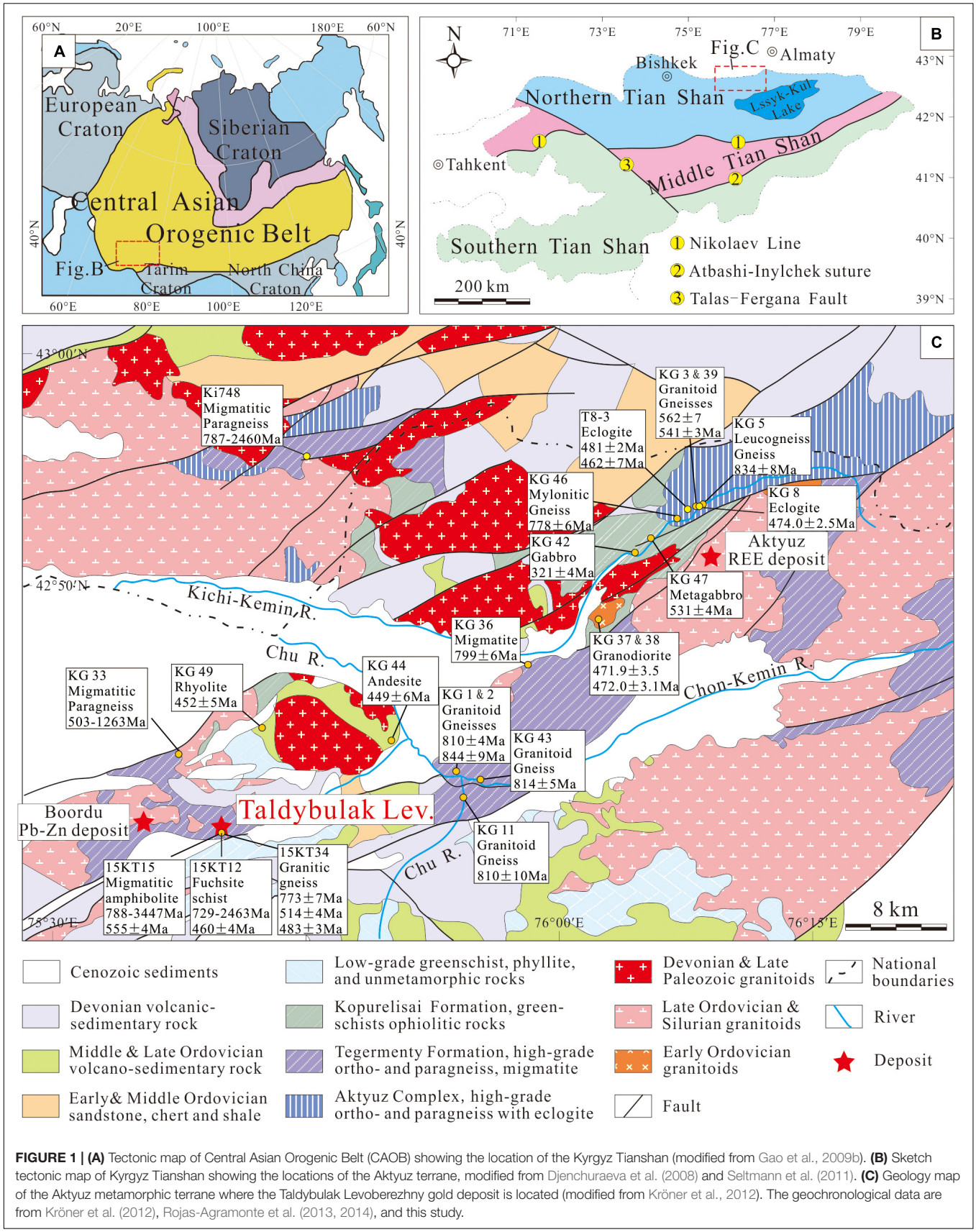

FIGURE 1 | (A) Tectonic map of Central Asian Orogenic Belt (CAOB) showing the location of the Kyrgyz Tianshan (modified from Gao et al., 2009b). **(B)** Sketch tectonic map of Kyrgyz Tianshan showing the locations of the Aktyuz terrane, modified from Djenchuraeva et al. (2008) and Seltmann et al. (2011). **(C)** Geology map of the Aktyuz metamorphic terrane where the Taldybulak Levoberezhny gold deposit is located (modified from Kröner et al., 2012). The geochronological data are from Kröner et al. (2012), Rojas-Agramonte et al. (2013, 2014), and this study.

enclosing layers or boudins of eclogite, garnet amphibolite, and amphibolite (Bakirov et al., 2003). The gneisses were previously considered to be Archean and Paleoproterozoic in age (Bakirov and Korolev, 1979; Kiselev et al., 1993), although Kröner et al. (2012) reported protolith ages of 541 − 562 and 778 − 834 Ma for granitoid gneisses. Orozbaev et al. (2010) emphasized that the Aktyuz eclogite is unusual in that they occur as remnants in mafic dykes that previously intruded the sedimentary protolith, instead of in rocks derived from oceanic crust. The eclogites had undergone peak metamorphism in the range of 550–670°C and 1.6–2.3 GPa (Orozbaev et al., 2010). Tagiri et al. (1995) obtained a mineral/whole-rock Rb–Sr isochron age of 749 ± 14 Ma for an eclogite sample, but this age is controversial. Rojas-Agramonte et al. (2013) and Klemd et al. (2014) reported Sm–Nd, Ar/Ar, and Lu–Hf ages of 462 ± 7 Ma, 481 ± 2 Ma, and 474.3 ± 2.2 Ma, respectively (**Supplementary Table 4**). Such ages are comparable with the muscovite Ar/Ar plateau age for the country rock gneiss (475.7 ± 5.5 and 470.6 ± 5.3 Ma; Kröner et al., 2012) and thus may be reasonable for the HP–UHP metamorphic event.

The Kemin Complex in the south of the terrane is distinguished from the Aktyuz Complex by the absence of HP–UHP metamorphic rocks. It was subdivided into three formations named Kopurelisai, Kapchigai, and Kokbulak by Bakirov et al. (2003) and Orozbaev et al. (2010) or two formations named Kopurelisai and Tegermenty (Djenchuraeva et al., 2008). In this article, the second classification scheme was adopted. The Kopurelisai Formation consists of massive but foliated isotropic hornblende gabbro, greenschist-facies metabasalt, locally with well-preserved but flattened pillows. It is in thrust contact along a serpentinite mélange zone with tectonically overlying gneiss of the Aktyuz Complex and interpreted as constituents of a dismembered ophiolite (Bakirov et al., 2003). Kröner et al. (2012) obtained a SHRIMP zircon U–Pb age of 531.2 ± 3.7 Ma for a foliated metagabbro. The Tegermenty Formation mainly consists of migmatitic paragneisses with subordinate granitoid gneisses. The matrix of some migmatites consists of amphibolitic gabbro, ultramafic rocks, and cherty schists, considered as a metamorphosed ophiolite by Bakirov et al. (2003). Previous α-Pb zircon dating yielded ages of 2,550 ± 250 and 2,050 ± 200 Ma for migmatitic gneisses (Bakirov and Korolev, 1979), whereas conventional multigrain U–Pb zircon dating of migmatitic tonalitic-trondhjemitic gneisses yielded ages of ∼2,050 and 1,850 ± 10 Ma (Kiselev et al., 1993). More precise geochronological data reported by Kröner et al. (2012) revealed protolith ages of 799 − 844 Ma for granitic gneiss and 503 − 2,460 Ma for paragneisses.

The Ordovician volcanic-sedimentary rocks unconformably overlying on the Kemin Complex are the oldest undeformed rocks in the region (**Figure 1C**). One rhyolite sample from the Burubai Formation yielded a SHRIMP zircon U–Pb age of 452.2 ± 2.8 Ma, and one porphyritic basaltic andesite from the Cholok Formation is nearly contemporaneous, aged 448.9 ± 5.6 Ma (Kröner et al., 2012). Devonian volcanic-sedimentary rocks in the southwest of the terrane are distributed around the metamorphic basement. Together they constitute the Taldybulak-Boordu dome (with an area of about 10 km × 20 km) that was subsequently intruded by the Late Paleozoic subvolcanic rocks.

DEPOSIT GEOLOGY AND SAMPLE DESCRIPTION

The Taldybulak Lev. gold deposit is located in the Taldybulak shear zone, which is an overthrust complex of highly deformed lithologies (Malyukova, 2001). The exposed strata include the Kopurelisai and Tegermenty Formations of the Kemin Complex and the volcanic-sedimentary rocks of the Devonian Barkol Formation (**Figure 2A**). The Kopurelisai Formation here is dominated by amphibolite, biotite amphibolite, schist, and migmatite, and the Tegermenty Formation consists mainly of mica schist with layers of gneiss and chert. The Devonian Barkol Formation unconformably covers the Tegermenty Formation metamorphic rocks. It is dominated by andesite, basaltic andesite, volcanic breccia, tuff, and sandstone (Djenchuraeva et al., 2008).

There are three shear and thrust zones in the mining area, which are successively named the Upper zone, the Middle zone, and the Taldybulak zone from west to east, with a total thickness of about 700 m (**Figures 2A,B**). In the shearing zone, there is a chaotic assemblage of schist, amphibolite, and gneisses that have undergone intensive quartz–calcite and quartz–sericite alteration. They were further offset by an NE-trending or nearly E–W-trending fault and intruded by numerous diorite-monzodiorite–monzogranite or dolerite dykes (Zhao et al., 2015, 2017).

Thus far, 11 gold ore bodies have been discovered, which are confined to the shear zone or around the granitic dykes (**Figures 2A,B**). The No. 1 orebody is a prominent entity located at the junction of the Taldybulak shear and thrust zone with a nearly E–W-trending fault. Its eastern area is vein- or pipe-shaped and decreases gradually to the west. It extends for ca. 1,300 m, and a width of 60 − 350 m and a thickness of 20 − 80 m (Xi et al., 2018). Except for Nos. I and II, other orebodies occur mainly as veins or lenses.

In this study, four samples, namely one auriferous porphyry and three wall rock samples from the Kopurelisai Formation, were selected for zircon U–Pb dating and Lu–Hf isotopic studies (**Figure 3**). Sample 15KT12 is a fuchsite schist collected from the No. 1582 ramp. It is dominated by quartz and fuchsite, where auriferous pyrite was associated with secondary sericite or calcite. Sample 15KT34 has little or no mineralization. It is a pink, medium-grained, finely layered granitic gneiss collected from the outcrops at the ventilation room of the deposit. It mainly consists of plagioclase, K-feldspar, biotite, quartz, and secondary sericite and epidoite. Sample15KT15 is a migmatitic amphibolite collected from the No. 1582 ramp. The matrix is gray or gray-green colored and consists mainly of hornblende, plagioclase, and biotite with volumetric percentages of 55, 40, and <5%, respectively. The hornblende was partially replaced by epidote, chlorite, calcite, and quartz. The leucosome is pink colored and contains mainly quartz, plagioclase, and K-feldspar. Sample 15KD66 is a medium-grained, reddish-colored biotite monzonite porphyry intruding the fuchsite schist. The sample

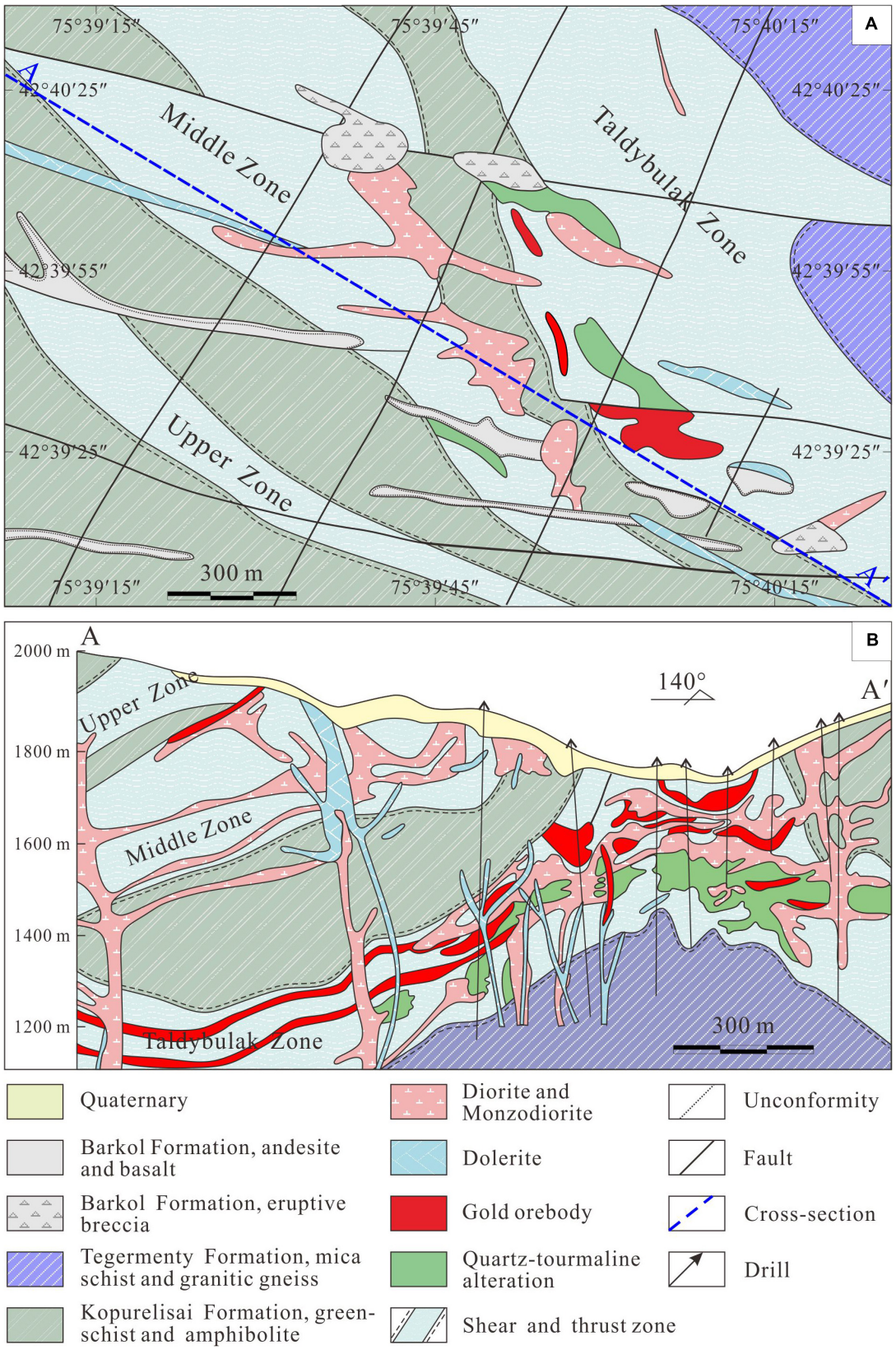

FIGURE 2 | Geological map **(A)** and a cross-section along A–A′ **(B)** of the Taldybulak Levoberezhny gold deposit, modified from Malyukova (2001) and Djenchuraeva et al. (2008).

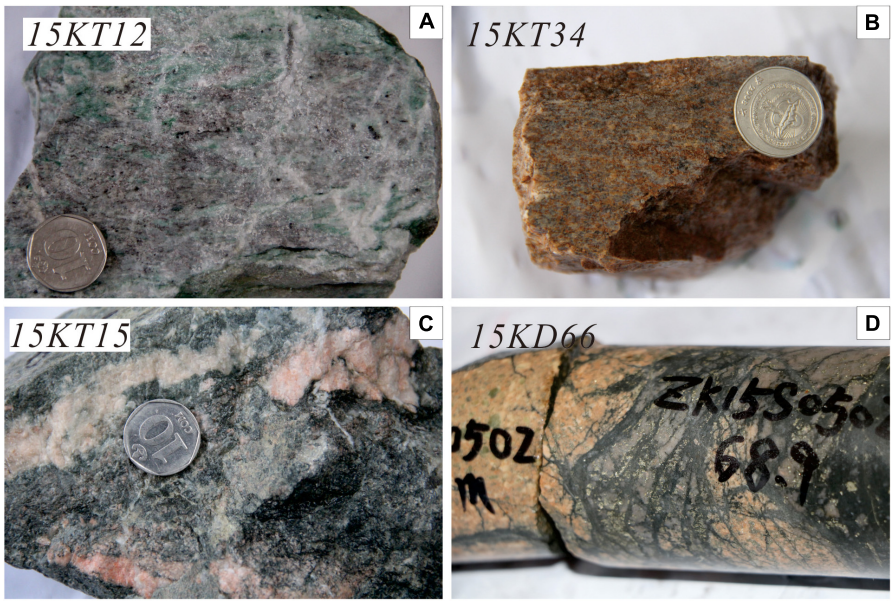

FIGURE 3 | Photographs showing samples used for geochronological study. **(A)** Fuchsite schist; **(B)** granitic gneiss; **(C)** migmatitic amphibolite; and **(D)** monzogranite porphyry.

was collected from drilling hole ZK15S0502 (with a sample depth of 68.9 m). It has a typical porphyritic texture, with plagioclase and K-feldspar phenocrysts in a groundmass of K-feldspar, plagioclase, quartz, biotite, and apatite. The auriferous porphyry was intensively altered by sericite and calcite, hosting abundant quartz–tourmaline–pyrite veins or veinlets (**Figure 3D**).

ANALYTICAL METHOD

In situ Zircon U–Pb Dating and Hf Isotopic Analyses

Zircon grains were extracted by magnetic techniques and conventional heavy liquids and then purified by handpicking under a binocular microscope. Representative zircon grains were mounted in epoxy resin and polished down to expose the grain center. Cathodoluminescence (CL) images of zircons were taken at the Beijing Zircon Linghang Technology Company, Beijing. The images were obtained by a MonoCL^{3+} (Gatan Company, Abingdon, England) CL spectroscope attached to a Quanta 400 FEG Scanning Electron Microscope. The operative condition during CL imaging was 15 kV.

In situ zircon laser ablation inductively coupled plasma-mass spectrometry (LA-ICPMS) U–Pb dating, Hf isotope, and trace element analyses were conducted at the State Key Laboratory of Continental Dynamics at Northwest University, Xi'an. The laser denudation system consists of a Geolas 2005 excimer ArF laser-ablation system (Lambda Physik AG, Göttingham, Germany), Elan 6100 DRC (Dynamic Reaction Cell) Q-ICP-MS (Inductively Coupled Plasma Mass Spectrometry, Perkin Elmer Lnc., United States of America), and Nu Plasma HR MC-ICP-MS (High Resolution Multiple Collector Inductively Coupled Plasma Mass Spectrometer, Nu Instruments Ltd., Wrexham, United Kingdom), which were used for simultaneous acquisition of trace elements, Hf isotopes, and U–Pb isotopes. The zircon aerosol generated by the laser was split into two transmission tubes by a y-shaped convection device after the ablation unit and introduced into two mass spectrometers at the same time. The hafnium isotopes were measured by MC-ICP-MS, and U–Pb age and trace element composition were measured by Q-ICP-MS. An Edwards E2M80 source rotary pump was used in the interface area to improve sensitivity. The spot size was 30 μm for U–Pb dating and 40 μm for Lu–Hf analysis. Helium was used as the carrier gas to provide effective aerosol transport to ICP and to minimize aerosol deposition. The detailed analytical procedure can be found in Yuan et al. (2008).

Standard Zircon GJ-1, 91500, NIST SRM 610, and Monasteries are used as reference standards for calibration and control of analytical instrument conditions. Uranium, lead, thorium, and trace element concentrations were calibrated using ^{29}Si as an internal standard and NIST SRM 610 as an external reference standard. ^{202}Hg in Q-ICP-MS gas blank is usually < 30. Therefore, the contribution of ^{204}Hg to ^{204}Pb is negligible and has not been adjusted. The ^{206}Pb/^{238}U, ^{207}Pb/^{206}Pb, ^{208}Pb/^{232}Th, and ^{207}Pb/^{235}U ratios were calculated using the GLITTER 4.4 (GEMOC, Macquarie University, Sydney, Australia), and zircon 91500 was used to correct instrument mass deviations and depth-dependent element and isotope fractionation. Zircon 91500 and GJ-1 is used as an external standard. Obtained ^{206}Pb/^{238}U weighted mean ages of 91,500 and GJ-1 were 1,062 ± 5.6 Ma (2σ) and 604.8 ± 5.6 Ma (2σ), respectively, highly consistent with the recommended ages. Common lead was corrected according to the method put forward by Andersen (2002). The results were reported as one error. The Concordia plot and

weighted average U–Pb age (95% confidence) were obtained using the ISOPLOT 3.0 (Ludwig, 2003).

Interference of $^{176}Lu/^{177}Hf$ was corrected by measuring the intensity of the ^{175}Lu without interference, and the $^{176}Lu/^{177}Hf$ was calculated using the recommended ratio of $^{176}Lu/^{175}Lu$ with 0.02669 (Horn and von Blanckenburg, 2007). In the same way, we used the recommended $^{176}Yb/^{177}Hf$ ratio of 0.5586 (Hazarika et al., 2018) to correct the $^{176}Yb/^{172}Yb$ ratio to calculate the $^{176}Yb/^{177}Hf$ ratio. In the course of analysis, the ratio of $^{176}Hf/^{177}Hf$ obtained in the analysis is 0.282296 ± 50 for 91,500 and 0.282019 ± 15 for GJ-1, consistent with the recommended ratios of 0.2823075 ± 58 and 0.282015, respectively. Analytical ratios of $^{176}Hf/^{177}Hf$, $^{176}Yb/^{177}Hf$, and $^{176}Lu/^{177}Hf$ are reported with 2σ error. The initial $^{176}Lu/^{177}Hf$ ratio is calculated based on chondrite simultaneously with zircon growth in magma. The decay constant of the chondritic ratios of $^{176}Lu/^{177}Hf$ with 0.282772, 1.867×10^{-11} for ^{176} Lu (SöDerlund et al., 2004) and $^{176}Lu/^{177}Hf$ with 0.0332 are introduced by Blichert-Toft and Albarède (1997). The current ratios of 0.28325 at $^{176}Lu/^{177}Hf$ and 0.0384 at $^{176}Lu/^{177}Hf$ are used to calculate single-stage Hf model ages (T_{DM1}) relative to the depleted mantle. The referred $^{176}Lu/^{177}Hf$ value with 0.0093 for average upper continental crust and the $f_{Lu/Hf}$ value of − 0.55 for the average continental crust are used to calculate two-stage Hf model ages (T_{DM2}) (Vervoort and Patchett, 1996; Vervoort and Blichert-Toft, 1999). The $f_{Lu/Hf}$ ratio equals $(^{176}Lu/^{177}Hf)_s/(^{176}Lu/^{177}Hf)_{CHUR} - 1$, where the $(^{176}Lu/^{177}Hf)_{CHUR}$ = 0.0332, and the $(^{176}Lu/^{177}Hf)_s$ value is obtained from analysis of the sample.

SIMS Zircon U–Pb Dating

To better constrain the ages of the rim or cores, zircon U–Pb dating of sample 15KT15 and 15KD66 was further conducted using a Cameca IMS-1280HR SIMS at the Institute of Geology and Geophysics, Chinese Academy of Sciences in Beijing. For comprehensive descriptions of the instrument and the analytical procedure, refer to Li et al. (2009). A brief summary is provided here. The primary O_2^- ion beam spot is about 20 μm × 30 μm in size, and positive secondary ions were extracted with a 10-kV potential. In the secondary ion beam optics, an energy window of 60 eV was used, together with a mass resolution of ca. 5,400 (at 10% peak height), to separate Pb^+ peaks from isobaric interferences. A single electron multiplier was used in the ion-counting mode to measure secondary ion beam intensities by peak jumping mode. Analyses of the standard zircon Plesovice were interspersed with unknown grains. Each measurement consists of seven cycles. Pb/U calibration was performed relative to zircon standard Plesovice ($^{206}Pb/^{238}U$ age = 337 Ma, Slama et al., 2008); U and Th concentrations were calibrated against zircon standard 91500 (Th = 29 ppm and U = 81 ppm; Wiedenbeck et al., 1995). A long-term uncertainty of 1.5% [1σ relative standard deviation (RSD)] for $^{206}Pb/^{238}U$ measurements of the standard zircons was propagated to the unknowns (Li et al., 2010), despite that the measured $^{206}Pb/^{238}U$ error in a specific session is generally ≤1% (1 σ RSD). The measured compositions were corrected for common Pb using non-radiogenic ^{204}Pb. Corrections are sufficiently small to be insensitive to the choice of common Pb composition, and an average of present-day crustal composition (Stacey and Kramers, 1975) is used for the common Pb assuming that the common Pb is largely surface contamination introduced during sample preparation. Data reduction was carried out using the ISOPLOT 3.0 (Ludwig, 2003). Uncertainties in individual analyses in data tables are reported at the 1σ level; Concordia U–Pb ages are reported with 95% CI, unless otherwise stated.

To monitor the external uncertainties of SIMS U–Pb zircon dating calibrated against a Plesovice standard, a standard zircon GBW04705 (Qinghu) was alternately analyzed as an unknown together with other unknown zircons. Nine measurements on Qinghu zircon yielded a Concordia age of 160 ± 1 Ma, which is identical within error to the recommended value of 159.5 ± 0.2 Ma (Li et al., 2013).

RESULTS

Zircon Morphology and U–Pb Ages

The zircon CL images, LA-ICPMS, and SIMS U–Pb data are available in **Supplementary Tables 1,2** and **Figures 4–6**. It is commonly accepted that precise dating of zircon crystals younger than 1,000 Ma is best achieved by using concordant $^{206}Pb/^{238}U$ age, whereas the older grains would be more precisely dated using $^{206}Pb/^{207}Pb$ ages due to decreasing amounts of radiogenic lead available for the measurement (Kröner et al., 2012; Rojas-Agramonte et al., 2013; Zhang et al., 2020).

Detrital zircons collected from sample 15KT12 are mainly light black and colorless, with lengths ranging from 80 to 280 μm and length/width ratios from 1.3:1 to 3:1. They tend to have near-euhedral to subhedral shapes, indicative of rather short transport and source areas not far from the depositional sites. The CL images illustrate that the zircons generally have complex inner textures, with a bright, oscillatory zoned core overgrown by a dark, unzoned rim (**Figure 4B**). Nineteen of 23 LA-ICPMS analyses were performed on the central part. They yielded highly variable U (36 − 1,393 ppm) and Th (30 − 250 ppm) contents as well as Th/U ratios (0.07 − 1.51) and provide an array of concordant or near-concordant data corresponding to ages between 729 and 2,463 Ma (**Figure 4A**). The most prominent concentrate emanates from those with oscillatory zoning (**Figure 4B**), with 12 data points yielding a weighted mean age of 740 ± 5 Ma ($^{206}Pb/^{238}U$ age, mean squared weighted deviation (MSWD) = 0.95). Another seven spots on the core yielded $^{206}Pb/^{207}Pb$ ages of ca. 1,065 Ma, 1,190 Ma, 1,647 Ma, and ca. 2,450 Ma (**Supplementary Table 1**). The overgrowth has unambiguously lower Th (12 − 104 ppm) content and Th/U ratios (0.03 − 0.09). Four data points collectively yielded a weighted mean age of 460 ± 4 Ma ($^{206}Pb/^{238}U$ age, MSWD = 0.15). This distribution (**Figures 4A–C**) suggests a Neoproterozoic-Cambrian age (most probably between 729 and 463 Ma) of deposition and the source terrane ranges in age from Neoproterozoic to Paleoproterozoic. The rock underwent metamorphism at 460 Ma.

In sample 15KT34, the zircon crystals are gray-white-colored short prismatic or subhedral crystal, with a common length of 100–180 μm and length/width ratio of 1.3:1 to 2.5:1. The CL

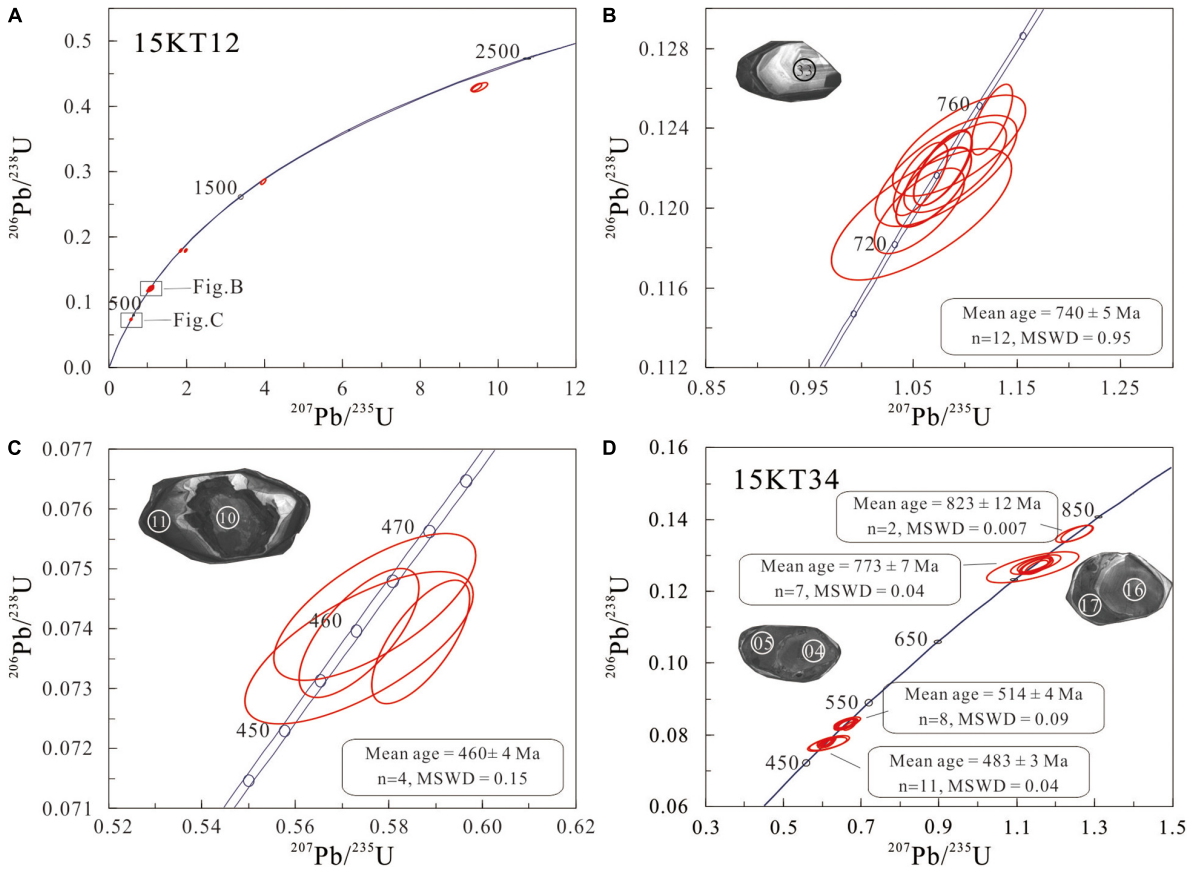

FIGURE 4 | U–Pb age Concordia plots for samples 15KT12 **(A–C)** and 15KT34 **(D)**. **(B,C)** are enlargements of **(A)**. Typical zircon cathodoluminescence (CL) images are also shown (the circle for LA-ICPMS dating is 30 μm).

imaging revealed that most zircon crystals contain inherited cores that can either be oscillatory zoned or exhibit faint zonation. Seventeen LA-ICPMS analyses on the interior reveal three populations. The older two populations have similar oscillatory zonation and overlapped U (105–299 ppm), Th (68–289 ppm), and Th/U ratios (0.46–1.16). Two analyses yielded an average of 823 ± 12 Ma (n = 2, MSWD = 0.007), and seven analyses yielded a younger age of 773 ± 7 Ma (n = 7, MSWD = 0.04). They are interpreted as the age of zircon xenocryst and the granitic protolith, respectively. The third population is easily distinguished by their unzoned or patch-zoned CL response and high U (388–558 ppm), but low Th (14–52 ppm) and Th/U ratios (0.03–0.11). They collectively give a weighted average age of 514 ± 4 Ma (n = 8, MSWD = 0.09) (**Figure 4D** and **Supplementary Table 1**), which may represent an important metamorphic event. Outward from the core is a dark overgrowth with little or no zonation. Eleven analyses reveal extremely low Th and Th/U ratios of 2–7 ppm and 0.01–0.03, respectively. Obtained $^{206}Pb/^{238}U$ ages vary from 481 ± 8 to 485 ± 5 Ma (1σ error), with a weighted average of 483 ± 3 Ma (n = 11, MSWD = 0.04). Furthermore, there is a very bright rim that is too thin to be dated precisely (**Figure 4D**).

In sample 15KT15, the zircon crystals have highly variable morphologies and colors (**Figures 5B–D**). Some grains are dark colored, subrounded columns, or almost spherical, whereas others are brown in color and subrounded to near-euhedral in shape. They range from 100 to 120 μm in length and 70 to 100 μm in width, yielding length/width ratios of 1.2:1 to 2:1. The CL images show that most zircons exhibit a distinct core–rim texture. In some cases, an inherited core is identified on the basis of its bright and well-round appearance, with oscillatory or planar zoning indicative of a magmatic origin. Interior domain mantling cores tend to be dark and unzoned in the CL response. They are further overgrown by thin, bright, and unzoned rims. A total of 50 LA-ICPMS analyses were conducted and provided mostly concordant, but highly diverse ages (**Figure 5A**). Eight core analyses yielded $^{206}Pb/^{238}U$ dates of 788–797 Ma and combined to a weighted average of 794 ± 5 Ma (n = 8, MSWD = 0.19). A second population on the core comprises 13 dates ranging from 931 to 948 Ma, with a weighted average of 941 ± 7 Ma (n = 13, MSWD = 2). Other spots on the core yielded ages ranging from 975 to 3,447 Ma (**Supplementary Table 1**). The youngest $^{206}Pb/^{238}U$ date averaged at 555 ± 4 Ma (n = 8, MSWD = 0.65) emanates from the thin zircon overgrowths that have low U (245–1,384 ppm, mostly < 500 ppm), extremely

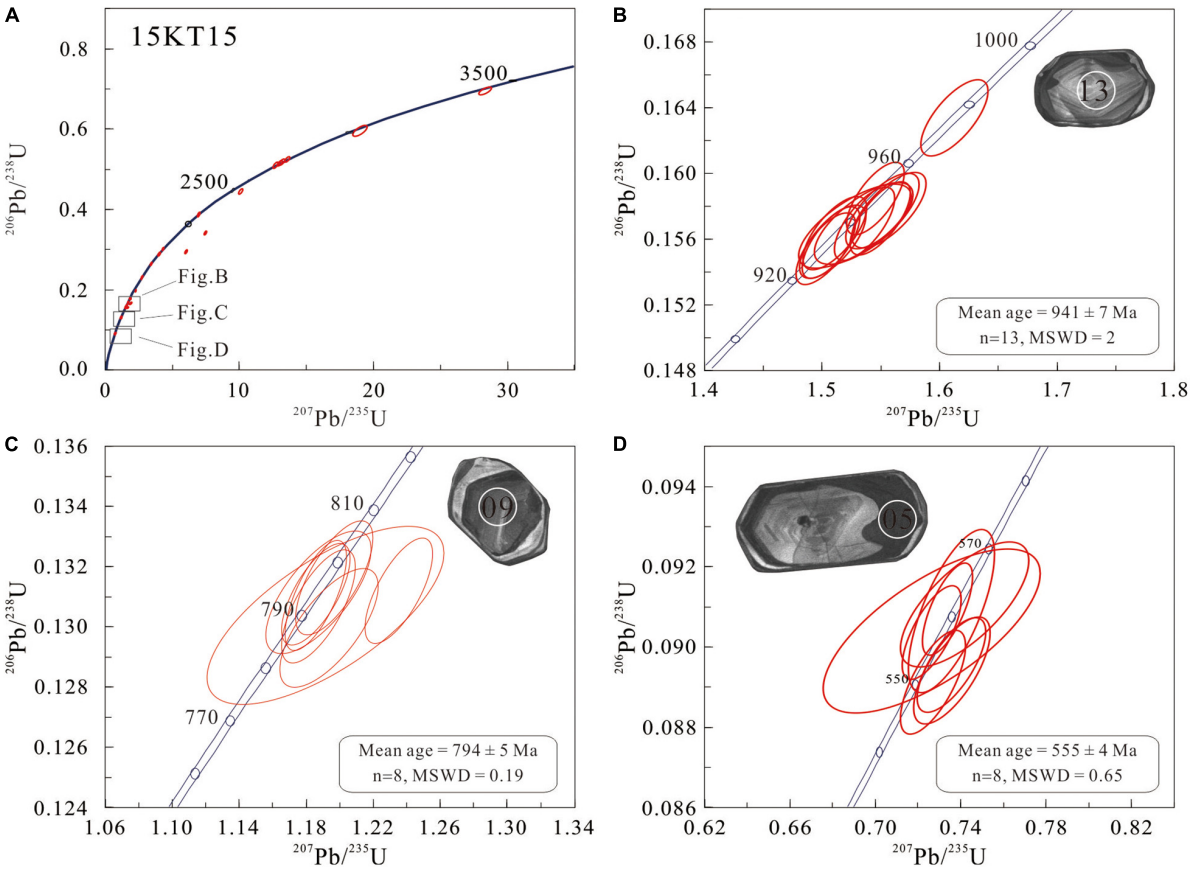

FIGURE 5 | U–Pb age Concordia plots for sample 15KT15. **(B–D)** are enlargements of **(A)**. Typical zircon cathodoluminescence (CL) images are also shown (the circle for LA-ICPMS dating is 30 μm).

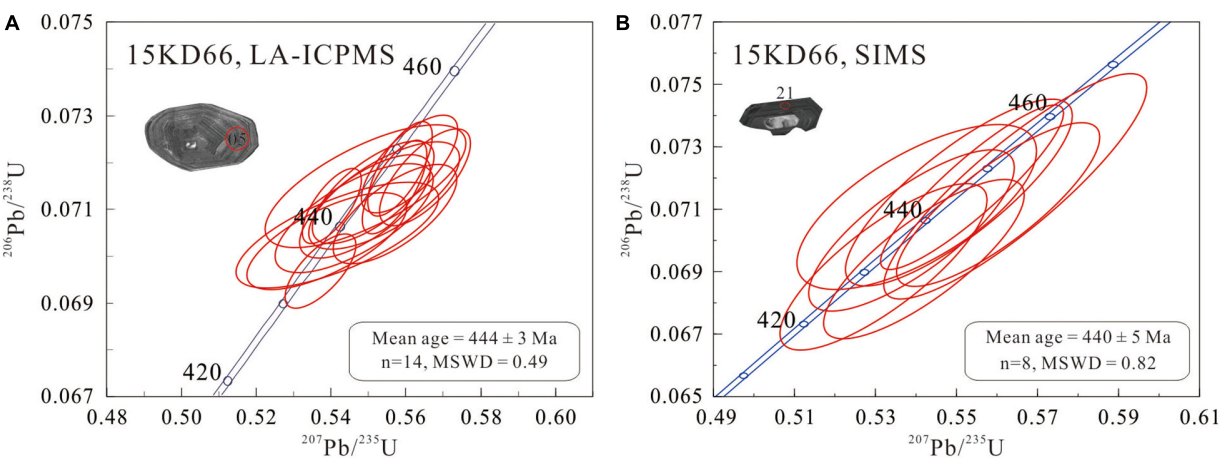

FIGURE 6 | U–Pb age Concordia plots for sample 15KD66, obtained by LA-ICPMS **(A)** and SIMS **(B)**, respectively. Typical zircon cathodoluminescence (CL) images are also shown (the circle for LA-ICPMS dating is 30 μm, for SIMS dating is 10 μm).

low Th (15–122 ppm, mostly < 35 ppm), and Th/U ratio (0.04–0.09). This could be regarded as the best estimate of an unbiased age for a metamorphic event. Furthermore, there is a rim, which is too thin to be dated precisely. The above result is further verified by an additional seven SIMS analyses that yielded consistent ages of 1,021 − 1,102 Ma, 895, 689, and 556 Ma (**Supplementary Table 2**). The youngest two ages averaged at 558 ± 12 Ma (MSWD = 0.03) may represent the

metamorphic event, whereas other older ages represent the ages of the sedimentary protolith.

Most zircon crystals collected from sample 15KD66 have an euhedral, elongated shape with sharp facets and pointed tips. The zircon crystals are mainly colorless and transparent, with lengths ranging from 140 to 270 μm and length/width ratios from 1.5:1 to 3:1. Occasionally, the prisms are irregular, suggesting chemical corrosion or physical abrasion. The CL investigation (**Figures 6A,B**) revealed that most zircon crystals have oscillatory zoning. Some grains have irregular cores mantled by oscillatory-zoned magmatic rims, and the core–rim boundary is often irregular and marked by a CL-bright thin band (**Figure 6B**). The cores are small (50–70 μm in length), with points being analyzed by LA-ICPMS. Three analyses on the inherited cores yielded ages of 766 ± 13, 770 ± 8, and 2,567 ± 35 Ma, respectively (**Supplementary Table 1**). In an attempt to date the crystallization age of the porphyry, the LA-ICPMS analyses were mainly concentrated on the zircon rims. A total of 14 analyses yielded consistent $^{206}Pb/^{238}U$ ages varying from 434 ± 7 to 448 ± 4 Ma, with a weighted mean of 444 ± 3 Ma (n = 14, MSWD = 0.49, **Figure 6A**). The same sample was further analyzed by SIMS. Nine analyses on the thin overgrowth yielded a weighted mean of 440 ± 5 Ma (n = 8, MSWD = 0.82, **Figure 6B**) that is indistinguishable from the LA-ICPMS data within error. Thus, the emplacement of the monzogranite porphyry is constrained to ca. 442 Ma.

Zircon Hf Isotopes

In sample 15KT12, three zircons belonging to the 740-Ma-aged group have $^{176}Lu/^{177}Hf$ ratios of 0.000232–0.000785, $^{176}Hf/^{177}Hf$ ratios of 0.281841–0.281963, εHf(t) values of − 17.0 to − 12.4, and two-stage Hf model ages (T_{DM2}) of 2,430–2,732 Ma. Another two zircons aged 1,193 and 2,463 Ma yielded higher $^{176}Lu/^{177}Hf$ ratios (0.001294 and 0.001248) but lower $^{176}Hf/^{177}Hf$ ratios (0.281680 and 0.280993) relative to the younger ones, with calculated εHf(t) of − 13.2 and − 9.8 and T_{DM2} ages of 2,813 and 3,563 Ma (**Figure 7** and **Supplementary Table 3**).

In sample 15KT34, the 773-Ma-aged zircons have $^{176}Lu/^{177}Hf$ ratios within a range between 0.000568 and 0.002407, $^{176}Hf/^{177}Hf$ ratios between 0.281681 and 0.281943, εHf(t) values between −22.8 and −12.8 and T_{DM2} ages between 2,469 and 3,088 Ma, respectively (**Figure 7** and **Supplementary Table 3**).

The zircons from the protolith of sample 15KT15 yielded a highly variable Hf isotopic composition. In general, the crystals aged 793 Ma have much lower $^{176}Hf/^{177}Hf$ ratios (0.281771 − 0.281963) and εHf(t) values (− 18.3 to − 11.5), but higher T_{DM2} ages (2,407 − 2,826 Ma) in comparison with the older group aged 941 Ma ($^{176}Hf/^{177}Hf$ = 0.281947–0.282269, εHf(t) = −8.5 to + 2.6, T_{DM2} = 1,634–2,335 Ma) (**Figure 7** and **Supplementary Table 3**).

Magmatic zircon rims from sample 15KD66 yielded slightly higher $^{176}Lu/^{177}Hf$ ratios (0.000730–0.002008) and T_{DM2} ages (1,908–2,197 Ma), but lower $^{176}Hf/^{177}Hf$ ratios (0.282162–0.282287) and εHf(t) values (from − 12.3 to − 7.7, **Figure 7** and **Supplementary Table 3**) compared with the inherited cores. Two 770-Ma-aged cores yielded $^{176}Lu/^{177}Hf$ ratios of 0.000177 and 0.000175, $^{176}Hf/^{177}Hf$ ratios of 0.282006 and 0.282009, εHf(t) values of − 10.3 and − 10.1, and T_{DM2} of 2,310 and 2,301 Ma. Another Archean aged core (2,567 Ma), however, has an even higher $^{176}Hf/^{177}Hf$ ratio of 0.280993, εHf(t) value of − 7.5 and T_{DM2} age of 3,503 Ma (**Figure 7** and **Supplementary Table 3**).

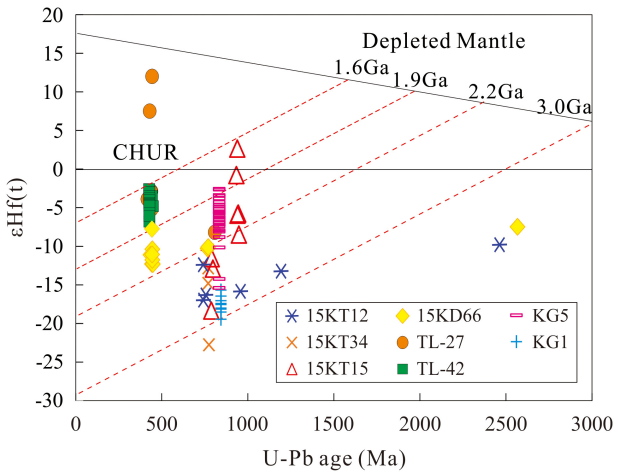

FIGURE 7 | εHf(t) vs. age plot showing most zircon samples from the Aktyuz Terrane with negative εHf(t) values. Samples: fuchsite schist (15KT12), granitic gneiss (15KT34), migmatitic amphibolite (15KT15), and gray granitoid gneiss (KG1, Kröner et al., 2012) of the Kemin Complex, well-banded leucogneiss (KG5, Kröner et al., 2012) of the Aktyuz Complex, and monzogranite porphyry (15KD66), diorite (TL-27, Zhao et al., 2017), and monzonite (TL-42, Zhao et al., 2017) outcropped in the Taldybulak Levoberezhny deposit.

DISCUSSION

Evidence for Porphyry-Type Gold Mineralization

Since its discovery in 1963, the ore genesis of the Taldybulak Lev. deposit has been hotly debated. Some scholars regard the deposit as a complex porphyry system (Trifonov, 1987; Malyukova, 2001; Djenchuraeva et al., 2008; Seltmann et al., 2014) based on the spatial association between the porphyritic dykes and gold mineralization revealed by extensive drilling in Soviet times (**Figure 2B**). Emplacement ages of these intrusions, however, are poorly constrained, with available ages varying considerably from 183 to 403 Ma (without dating error, K–Ar dating). By contrast, Xue et al. (2014) and Goldfarb et al. (2014) proposed that the deposit may be orogenic gold system considering that it is spatially controlled by the shear and thrust zones. Zhao et al. (2015, 2017) suggested a multistage mineralization involving both orogenic and porphyry events and provided two sulfide Re–Os isochron ages of 434 ± 18 Ma (n = 6, MSWD = 24) and 511 ± 18 Ma (n = 5, MSWD = 2.0). Thus, the emplacement age of the granitic dyke and its contribution to gold mineralization becomes a key point.

In this article, one monzogranite sample with crosscutting quartz–tourmaline–pyrite veinlets was collected. The rock was intensively altered, with typical porphyry-type alterations including silicic, potassic, and sericite alterations.

Djenchuraeva et al. (2008) further proposed a vertically zoned hydrothermal alteration surrounding the diorite–monzonite intrusion, including the argillic zone corresponding to the apical part, the quartz–carbonate, and quartz–sericite zones around the intrusion, grading at depth to potassic alteration and the quartz–tourmaline alteration. Detailed petrological studies revealed native gold and electrum (with gold contents of 76.51%) inclusions in pyrite, and the pyrite itself contains considerable invisible gold up to 0.26% (Xi et al., 2018). Our new U–Pb ages provide a robust geochronological constraint for the emplacement of the auriferous monzogranite porphyry (**Supplementary Table 1**), with overlapping ages of 444 ± 3 Ma (n = 14, MSWD = 0.93) and 440 ± 4 Ma (n = 9, MSWD = 6.5) revealed by LA-ICPMS and SIMS U–Pb dating, respectively. These ages are consistent with the sulfide Re–Os isochron age of 434 ± 18 Ma (n = 6, MSWD = 24, Zhao et al., 2015) within error, providing another line of evidence for porphyry mineralization.

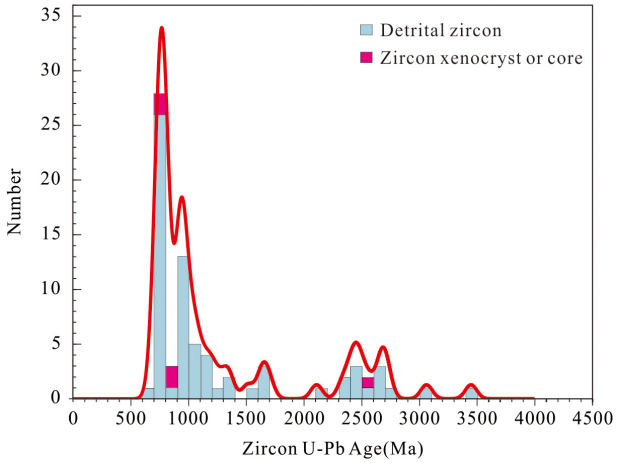

FIGURE 8 | Probability plot of detrital and xenocryst zircons from samples 15KT12, 15KT34, 15KT15, and 15KD66.

The Age and Reworking of the Precambrian Basement

The Kyrgyz North Tianshan, including the Aktyuz terrane, is one of the oldest orogenic domains of the CAOB. It has a Precambrian block mainly consisting of Grenvillian-aged granitoids, whereas the subordinate Paleoproterozoic and Archean rocks crop out in its western extension to southern Kazakhstan (Kröner et al., 2014). Based on detrital and xenocryst zircon ages and comparison with published ages from the Chinese Tianshan and the Tarim Craton, Rojas-Agramonte et al. (2014) suggested that the Kyrgyz North Tianshan rifted off the Tarim craton.

In this study, the inhomogeneous population of zircons from the fuchsite schist and migmatitic amphibolite supports a detrital origin of the zircons. These zircons are mostly near-euhedral to subhedral in shape, with a few exhibiting slight rounding at their terminations, suggesting a relatively short transport and source areas not far from the depositional site. As shown in the age probability plot (**Figure 8**), the most prominent age frequency is bracketed between 700 and 1,200 Ma. Such a major phase of Neo- to Mesoproterozoic magmatic event is not only prevalent in North Tianshan, but also well documented in surrounding areas such as Kyrgyz Middle Tianshan, southern Kazakhstan, the Chinese Tianshan, and the Tarim Craton (Kiselev and Maksumova, 2001; Kröner et al., 2007; Zhou et al., 2017, 2018). Another main cluster of single grain U–Pb ages between 2,300 and 2,700 Ma accords well with the Paleoproterozoic to Neoarchean peaks revealed by detrital and xenocryst zircons from the North Tianshan, South Tianshan, and the Tarim craton (Rojas-Agramonte et al., 2014). A minor peak between 1,500 and 1,700 Ma is difficult to interpret because it corresponds to the global magmatic hiatus (Condie and Aster, 2010). The oldest zircon age is 3,447 ± 32 Ma, suggesting the presence of Archean crust.

The old zircon cores or xenocryst also carry a record of older geological history, signifying the existence of a Precambrian basement at depth. In the monzogranite porphyry, three zircon cores yielded concordant ages of 766, 770, and 2,567 Ma, respectively. In the case of granitic gneiss, there are two xenocrysts aged at ca. 823 Ma. The younger ages grouped at 770–823 Ma fit well to the Neoproterozoic peak for detrital zircons, whereas the old age of 2,567 Ma corresponds to the Archean peak around 2,500 Ma (**Figure 8**). Zircon xenocrysts of similar ages are also reported for other rocks in this region. For instance, Zhao et al. (2017) reported two inherited zircon aged 813 and 808 Ma from a diorite outcropped in the deposit. Kröner et al. (2012) recognized zircon xenocrysts dated at 1,180 Ma in a Neoproterozoic migmatite of the Kemin Complex and at 1,263 Ma in a para-migmatite sample.

More evidence for an early Archean crustal component is presented based on our zircon Lu–Hf isotope studies of monzogranite porphyry and other detrital zircons. In the former case, 26 out of 27 zircons yielded negative εHf(t) values between − 22.8 and − 0.8 (**Figure 7**), with one exceptional positive εHf(t) value of 2.6. Zhao et al. (2017) carried out zircon Lu–Hf isotopic studies for one diorite (435.3 ± 3.8 Ma) and one monzogranite (427.7 ± 1.9 Ma) sample of similar ages. Their results yielded slightly higher εHf(t) values (− 8.2 to 12), with data varying between negative and positive. The Neoproterozoic granitoids outcropped in the Aktyuz terrane yielded even lower negative εHf(t) values indicative of crustal remelting. Kröner et al. (2012) obtained zircon εHf(t) values of − 19.5 to − 15.7 for a gray granodioritic gneiss (844 ± 9 Ma) of the Kemin Complex, and − 15.4 to − 2.6 for a well-banded leucogneiss (834 ± 8 Ma) of the Aktyuz Complex. Such highly evolved εHf(t) values, in combination with geochemistry and whole-rock Sr–Nd isotopic data (Kröner et al., 2012; Zhao et al., 2017), reveal that at least the Paleozoic and Neoproterozoic magmatic rocks outcropped in the Aktyuz terrane mainly resulted from partial melting of continental crust or its mixing with limited juvenile or short-lived material. This supports the conclusion proposed by Kröner et al. (2013) that the production of mantle-derived or juvenile continental crust in CAOB has been overstated. The results also provide clues that there is

an extensive Precambrian basement at depth, more than the surface outcrops; the Aktyuz terrane consists of reworked crustal material, some of it with a long history, possibly dating back to the Archean Eon.

The Timing of Metamorphism and Its Geological Significance

No geochronological constraint had been available for the metamorphism of the Kemin Complex until the present study. Our work reveals zircon overgrowth with a low Th/U ratio (generally < 0.1, **Supplementary Table 1**) and unzoned or patch-zoned CL imaging. They generally grow surrounding an oscillatory-zoned core and are attributed to a metamorphic origin according to Corfu et al. (2003) and Wu and Zheng (2004). Such overgrowths yielded a weighted mean of 460 ± 4 Ma for fuchsite schist, indicating a Middle Ordovician metamorphic event. The migmatitic amphibolite, by contrast, exhibits Neoproterozoic metamorphism at 555 ± 4 Ma, although a subsequent metamorphic event cannot be excluded since the ca. 555-Ma-aged overgrowth still has a distinct bright, thin rim (**Figure 5D**). Interestingly, the granitic gneiss experienced two metamorphic events at ca. 514 Ma and 483 Ma that can even be recorded by a single zircon grain (the left one in **Figure 5D**). Hence, the above data reveal that both a Neoproterozoic-Cambrian (514 – 555 Ma) and an Ordovician (460 – 483 Ma) metamorphism were accompanied by zircon growth. The latter matches well with the timing of HP–UHP metamorphism of the Aktyuz Complex (462–481 Ma, by Sm–Nd, Lu–Hf, and Ar/Ar dating, **Supplementary Table 4**), but no precursor metamorphic event has been reported for the Aktyuz Complex. Instead, the Neoproterozoic-Cambrian metamorphic event is in good agreement with the HP–UHP metamorphism at other complexes such as Kokchetav, Makbal, and Anrakhai.

At the Kokchetav Terrane, northern Kazakhstan, the HP–UHP metamorphism and subsequent exhumation are well confined to 530 – 540 Ma and 505 – 530 Ma by biotite Ar/Ar and zircon U–Pb dating (Claoué-Long et al., 1991; Shatsky et al., 1999; Hermann et al., 2001; Dobretsov et al., 2005, 2006; Buslov et al., 2010). The migmatites and gneisses within the terrane (Katayama et al., 2001; Ragozin et al., 2009) yielded zircon U–Pb ages of 505 – 540 Ma, with the oldest and youngest being interpreted as the timing of peak metamorphism and the timing of UHP exhumation, respectively. The subsequent collisional deformation occurred at 470–490 Ma, inducing folding, shearing, and retrograde metamorphism (De Grave et al., 2006; Dobretsov and Buslov, 2007; Zhimulev et al., 2011). At the Makbal block of the Kyrgyz North Tianshan, the HP–UHP event was constrained to 480 – 509 Ma by monazite and zircon U–Pb dating (Togonbaeva et al., 2009; Konopelko et al., 2012). In the case of the Anrakhai Complex, SHRIMP zircon U–Pb dating yielded ages of ca. 490 Ma for garnet pyroxenite, constraining a Late Cambrian HP metamorphism and exhumation (Alexeiev et al., 2011). These lines of geochronological evidence support a possible link among these terranes and support a Kokchetav–Kyrgyz North Tianshan belt (Windley et al., 2007; Kröner et al., 2012).

Tectonic Evolution and the Fate of the Gold Deposit

The current geodynamic model for the Aktyuz terrane (Alexeiev et al., 2011; Kröner et al., 2012; Rojas-Agramonte et al., 2013) favors the North Tianshan as a microcontinent sandwiched between the Dzhalair-Naiman basin in the north and the Kyrgyz-Terskey basin in the south during the Cambrian and Early Ordovician. Our new data, in combination with previous results (Kröner et al., 2012; Rojas-Agramonte et al., 2013, 2014), reveal a Precambrian basement that shows affinity to other small fragments in the Kokchetav–North Tianshan belt. The Aktyuz terrane itself, however, is not a coherent continental domain, but instead, is composed of tectonic slivers including Precambrian continental crusts and Early Paleozoic ophiolite. This is also evident in the variable Hf isotope of the Kemin and Aktyuz Complexes (**Figure 7**).

The southwest-directed subduction of the Paleo-Asian Ocean beneath the North Tianshan induced the opening of the Dzhalair-Naiman back-arc basin. The zircon U–Pb data of 531.2 ± 3.7 Ma (Kröner et al., 2012) for a leucogabbro sample from the Kopurelisai ophiolite suite confirms an Early Cambrian age (Ryazantsev et al., 2009). Although there are no available geochronological data, the massive sulfide ores of the Taldybulak Lev. deposit (Xi et al., 2018) may be the product of back-arc extension (**Figure 9**). It is hosted by the Kopurelisai Formation and underwent orogenic deformation. The sulfide Re–Os isochron of 511 ± 18 Ma that is interpreted as the timing of orogenic-type mineralization (Zhao et al., 2015, 2017) may alternatively record an initial massive sulfide precursor. The large uncertainty in this date prevents a comprehensive understanding of its geological meaning. Another response to the oceanic subduction is the granitoids with continental arc affinity. Kröner et al. (2012) reported zircon U–Pb ages of 541–562 Ma for the youngest granitoid gneisses at the Aktyuz terrane, which is comparable to a metadacite sample from the Anrakhai area. The Cambrian metamorphic zircon overgrowth recognized in our study may evidence this convergence. These rocks represent exotic slivers that share a similar metamorphic history with the Makbal or Kokchetav terranes.

Subsequent northwards subduction of the Dzhalair-Naiman basin and its final closure led to the convergence of the Anrakhai and Aktyuz microcontinents (Kröner et al., 2012). The previous passive margin of the North Tianshan microcontinent was involved in subduction underneath the Anrakhai microcontinent. Klemd et al. (2014) suggest that the HP rocks of the Aktyuz Complex represent subducted continental crust, and the eclogite and hosting metasedimentary rocks underwent metamorphism at variable depths of the subduction zone and subsequently juxtaposed during exhumation in the subduction channel. Our present study, in combination with previous stratigraphic, structural, and isotopic data (Kröner et al., 2012 and references therein), constrains the timing of the collision to Early Ordovician (most probably between 480 and 460 Ma). The Silurian (428–440 Ma) diorite and monzogranite outcropped in the Taldybulak Lev. deposit may be formed by partial melting of continental crust in a post-collision setting (Zhao et al., 2017).

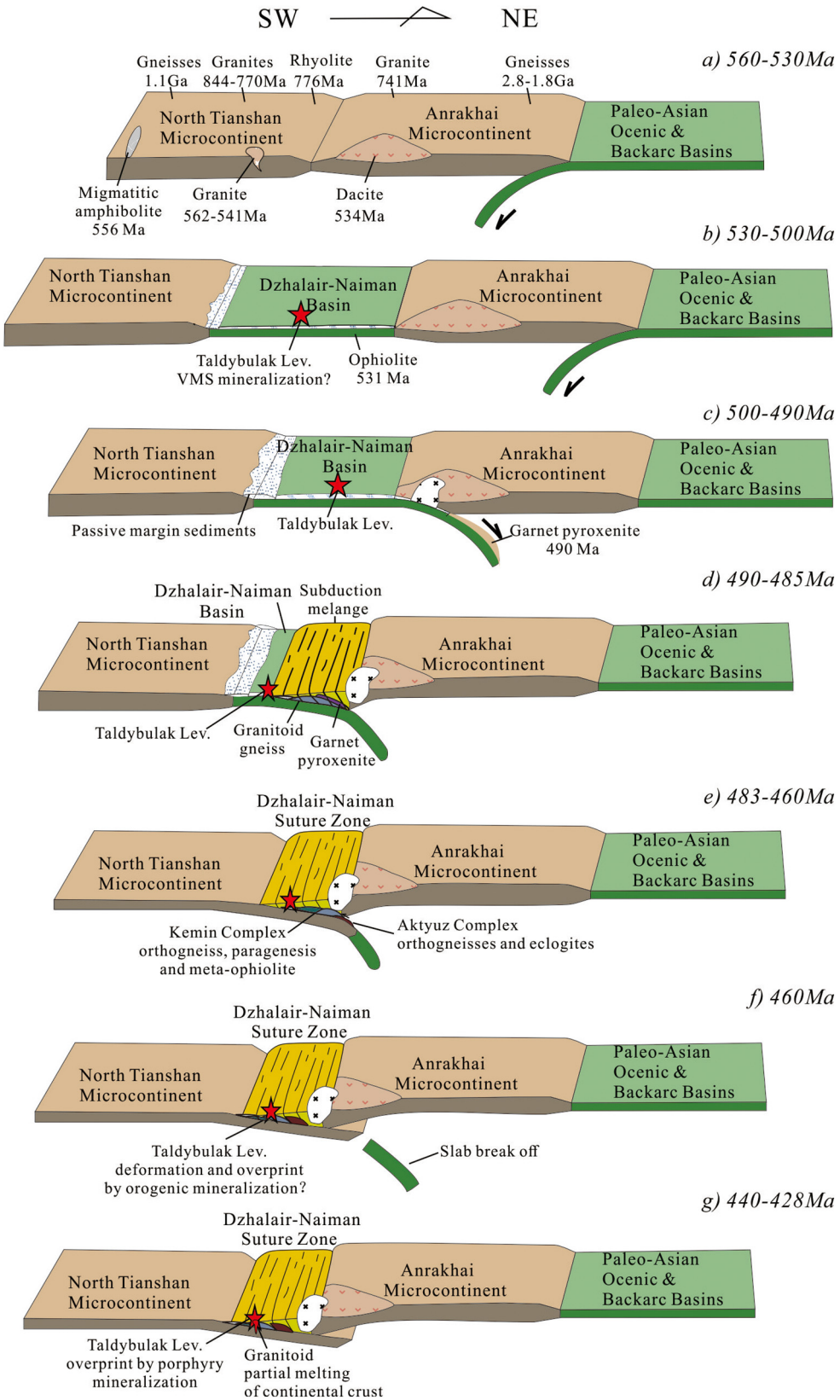

FIGURE 9 | Tectonic evolution of the Aktyuz Terrane and the fate of the Taldybulak Levoberezhny deposit (modified from Kröner et al., 2012).

They intruded into the metamorphic rocks, induced porphyry-type gold mineralization that superimposed on earlier VMS, and/or orogenic gold mineralization.

CONCLUSION

(1) The ore-causative monzogranite porphyry at the Taldybulak Lev. deposit was dated at 440 Ma.
(2) Three wall rock samples of the Kemin Complex yielded two episodes of metamorphic ages at 514 − 556 and 460 − 483 Ma, which may represent the age of oceanic subduction and continental collision, respectively.
(3) The detrital and xenocryst zircons (689 − 3,447 Ma), and highly evolved εHf(t) values (− 20.9 to − 7.8) and old two-stage Hf model ages (1,367 − 3,159 Ma), reveal the presence of a Precambrian basement that may be dated back to the Archean Eon.

DATA AVAILABILITY STATEMENT

The original contributions presented in the study are included in the article/**Supplementary Material**, further inquiries can be directed to the corresponding author/s.

AUTHOR CONTRIBUTIONS

WX provided initial data as part of a Ph.D thesis. NL and XX designed the project, and took the lead on writing the manuscript. XL and YW helped with the SIMS and LA-ICPMS dating. All authors contributed to the article and approved the submitted version.

FUNDING

This research was financially supported by the National Key Research and Development Program of China (No. 2017YFC0601202) and a Xinjiang Outstanding Youth Scientific Grant (No. 2020Q006).

ACKNOWLEDGMENTS

We are grateful to XD (the handling editor) and the two reviewers for their constructive comments and suggestions.

SUPPLEMENTARY MATERIAL

The Supplementary Material for this article can be found online at: https://www.frontiersin.org/articles/10.3389/feart.2021.664361/full#supplementary-material

Supplementary Table 1 | LA-ICPMS zircon U–Pb data for samples from the porphyry and metamorphic rocks.

Supplementary Table 2 | SIMS zircon U–Pb data for samples from the porphyry and metamorphic rocks.

Supplementary Table 3 | Zircon Lu–Hf isotope data for samples from the porphyry and wall rocks.

The following parameters were employed in the calculation: $(^{176}Lu/^{177}Hf)_{CHUR} = 0.0332$, $(^{176}Hf/^{177}Hf)_{CHUR,0} = 0.282772$, $(^{176}Lu/^{177}Hf)_{DM} = 0.0384$, $(^{176}Hf/^{177}Hf)_{DM,0} = 0.28325$ (Blichert-Toft and Albarède, 1997); $^{176}Lu/^{177}Hf$ for the average upper continental crust is 0.0093 (Vervoort and Patchett, 1996; Vervoort and Blichert-Toft, 1999); ^{176}Lu decay constant $\lambda = 1.867 \times 10^{-11}$ a^{-1} (SöDerlund et al., 2004).

Supplementary Table 4 | Available geochronological data from rocks from the Aktyuz terrane.

REFERENCES

Alexeiev, D. V., Kröner, A., Hegner, E., Rojas-Agramonte, Y., Biske, Y. S., Wong, G., et al. (2016). Middle to late Ordovician arc system in the Kyrgyz middle tianshan: from arc-continent collision to subsequent evolution of a Palaeozoic continental margin. *Gondwana Res.* 39, 261–291. doi: 10.1016/j.gr.2016.02.003

Alexeiev, D. V., Kröner, A., Kovach, V. P., Tretyakov, A. A., Rojas-Agramonte, Y., Degtyarev, K. E., et al. (2019). Evolution of cambrian and early ordovician arcs in the Kyrgyz North Tianshan: insights from U-Pb zircon ages and geochemical data. *Gondwana Res.* 66, 93–115. doi: 10.1016/j.gr.2018.09.005

Alexeiev, D. V., Ryazantsev, A. V., Kröner, A., Tretyakov, A. A., Xia, X., and Liu, D. Y. (2011). Geochemical data and zircon ages for rocks in a high-pressure belt of Chu-Yili mountains, southern Kazakhstan: implications for the earliest stages of accretion in Kazakhstan and the Tianshan. *J. Asian Earth Sci.* 42, 805–820. doi: 10.1016/j.jseaes.2010.09.004

Andersen, T. (2002). Correction of common lead in U-Pb analyses that do not report ^{204}Pb. *Chem. Geol.* 192, 59–79. doi: 10.1016/S0009-2541(02)00195-X

Bakirov, A. B., and Korolev, V. G. (1979). The age of oldest rocks in Tianshan. *Izvestiya AN SSSR Geol. Ser.* 7, 15–25.

Bakirov, A. B., Tagiri, M., Sakiev, K. S., and Ivleva, E. A. (2003). The lower precambrian rocks in the Tien Shan and their geodynamic setting. *Geotectonics* 37, 368–380.

Blichert-Toft, J., and Albarède, F. (1997). The Lu-Hf isotope geochemistry of chondrites and the evolution of the mantle-crust system. *Earth Planet. Sci. Lett.* 148, 243–258. doi: 10.1016/s0012-821x(97)00040-x

Buslov, M. M., Zhimulev, F. I., and Travin, A. V. (2010). New data on the structural setting and 40Ar/39Ar age of the MP-LP metamorphism of the Daulet formation, Kokchetav metamorphic belt, Northern Kazakhstan, and their tectonic interpretation. *Doklady Earth Sci.* 434, 1147–1151. doi: 10.1134/S1028334X10090023

Charvet, J., Liangshu, S., and Laurent-Charvet, S. (2007). Paleozoic structural and geodynamic evolution of eastern Tianshan (NW China): welding of the Tarim and Junggar Plates. *Episodes* 30, 162–186.

Charvet, J., Shu, L., Laurent-Charvet, S., Wang, B., Faure, M., Cluzel, D., et al. (2011). Palaeozoic tectonic evolution of the Tianshan belt, NW China. *Sci. China Earth Sci.* 54, 166–184. doi: 10.1007/s11430-010-4138-1

Chen, Y. J., Pirajno, F., Wu, G., Qi, J. P., and Xiong, X. L. (2012). Epithermal deposits in North Xinjiang, NW China. *Intern. J. Earth Sci.* 101, 889–917. doi: 10.1007/soo531-011-0689-4

Claoué-Long, J. C., Sobolev, N. V., Shatsky, V. S., and Sobolev, A. V. (1991). Zircon response to diamond-pressure metamorphism in the Kokchetav Massif, USSR. *Geology* 19, 710–713. doi: 10.1130/0091-76131991019<0710:ZRTDPM<2.3.CO;2

Condie, K. C., and Aster, R. C. (2010). Episodic zircon age spectra of orogenic granitoids: the supercontinent connection and continental growth. *Precamb. Res.* 180, 227–236. doi: 10.1016/j.precamres.2010.03.008

Corfu, F., Hanchar, J. M., Hoskin, P. W., and Kinny, P. (2003). Atlas of zircon textures. *Rev. Mineral. Geochem.* 53, 469–500. doi: 10.2113/0530469

De Grave, J., Buslov, M. M., Zhimulev, F., Vermeesch, P., Mcwilliams, M. O., and Metcalf, J. (2006). The Early Ordovician age of deformations in the Kokchetav

subduction-collision zone: new structural and Ar-40/Ar-39 data. *Russian Geol. Geophys.* 47, 441–450.

De Grave, J., Glorie, S., Buslov, M. M., Stockli, D. F., Mcwilliams, M. O., Batalev, V. Y., et al. (2013). Thermo-tectonic history of the Issyk-Kul basement (Kyrgyz Northern Tien Shan, Central Asia). *Gondwana Res.* 23, 998–1020. doi: 10.1016/j.gr.2012.06.014

Djenchuraeva, R. D., Borisov, F. I., Pak, N. T., and Malyukova, N. N. (2008). Metallogeny and geodynamics of the Aktiuz-Boordu mining District, Northern Tien Shan, Kyrgyzstan. *J. Asian Earth Sci.* 32, 280–299. doi: 10.1016/j.jseaes.2007.10.019

Dobretsov, N. L., and Buslov, M. M. (2007). Late cambrian-Ordovician tectonics and geodynamics of Central Asia. *Russian Geol. Geophys.* 48, 71–82. doi: 10.1016/j.rgg.2006.12.006

Dobretsov, N. L., Buslov, M. M., and Zhimulev, F. I. (2005). Cambrian-Ordovician tectonic evolution of the Kokchetav metamorphic belt, northern Kazakhstan. *Russian Geol. Geophys.* 46, 785–795.

Dobretsov, N. L., Buslov, M. M., Zhimulev, F. I., Travin, A. V., and Zayachkovky, A. A. (2006). Vendian-Early Ordovician geodynamic evolution and model for exhumation of ultrahigh- And high-pressure rocks from the Kokchetav subduction-collision zone. *Russian Geol. Geophys.* 47, 428–444.

Gao, J., and Klemd, R. (2003). Formation of HP-LT rocks and their tectonic implications in the western Tianshan Orogen, NW China. *Geochem. Age Const. Lithos.* 66, 1–22. doi: 10.1016/S0024-4937(02)00153-6

Gao, J., Long, L., Klemd, R., Qian, Q., Liu, D., Xiong, X., et al. (2009a). Tectonic evolution of the South Tianshan orogen and adjacent regions, NW China: geochemical and age constraints of granitoid rocks. *Intern. J. Earth Sci.* 98, 1221–1238. doi: 10.1007/s00531-008-0370-8

Gao, J., Qian, Q., Long, L. L., Zhang, X., Li, J. L., and Su, W. (2009b). Accretionary orogenic process of Western Tianshan, China. *Geol. Bull. China* 28, 1804–1816.

Glorie, S., De Grave, J., Buslov, M., Elburg, M., Stockli, D., and Gerdes, A. (2010). Multi-method chronometric constraints on the evolution of the Northern Kyrgyz Tien Shan granitoids (Central Asian Orogenic Belt): from emplacement to exhumation. *J. Asian Earth Sci.* 38, 131–146. doi: 10.1016/j.jseaes.2009.12.009

Goldfarb, R. J., Taylor, R. D., Collins, G. S., Goryachev, N. A., and Orlandini, O. F. (2014). Phanerozoic continental growth and gold metallogeny of Asia. *Gondwana Res.* 25, 48–102. doi: 10.1016/j.gr.2013.03.002

Han, B. F., He, G. Q., Wang, X. C., and Guo, Z. J. (2011). Late Carboniferous collision between the Tarim and Kazakhstan-Yili terranes in the western segment of the South Tian Shan Orogen, Central Asia, and implications for the Northern Xinjiang, western China. *Earth Sci. Rev.* 109, 74–93. doi: 10.1016/j.earscirev.2011.09.001

Hazarika, P., Mishra, B., and Lochan Pruseth, K. (2018). Trace-element geochemistry of pyrite and arsenopyrite: ore genetic implications for late Archean orogenic gold deposits in southern India. *Mineral. Magaz.* 81, 661–678. doi: 10.1180/minmag.2016.080.128

Hermann, J., Rubatto, D., Korsakov, A., and Shatsky, V. S. (2001). Multiple zircon growth during fast exhumation of diamondiferous, deeply subducted continental crust (Kokchetav Massif, Kazakhstan). *Contribut. Mineral. Petrol.* 141, 66–82. doi: 10.1007/s004100000218

Horn, I., and von Blanckenburg, F. (2007). Investigation on elemental and isotopic fractionation during 196 nm femtosecond laser ablation multiple collector inductively coupled plasma mass spectrometry. *Spectrochim. Acta Part B Atom. Spectrosc.* 62, 410–422. doi: 10.1016/j.sab.2007.03.034

Katayama, I., Maruyama, S., Parkinson, C. D., Terada, K., and Sano, Y. (2001). Ion micro-probe U-Pb zircon geochronology of peak and retrograde stages of ultrahigh-pressure metamorphic rocks from the Kokchetav massif, northern Kazakhstan. *Earth Planet. Sci. Lett.* 188, 185–198. doi: 10.1016/S0012-821X(01)00319-3

Kiselev, V., Apayarovm, F. K. M., Komarevtsev, E. N., Tsyganok, E. N., and Lukashova, E. M. (1993). "Zircon isotopic ages of crystalline complexes of Tien-Shan," in *Early Precambrian of the Central Asian Fold Belt*, ed. I. K. Kazakov (St. Petersbrug: Nauka), 99–115.

Kiselev, V., and Maksumova, R. (2001). Geology of the Northern and Middle Tien Shan: principal outlines. Paleozoic geodynamics and Gold Deposits in the Kyrgyz Tien Shan. *IAGOD Guidebook Ser.* 9, 21–28.

Klemd, R., Brocker, M., Hacker, B. R., Gao, J., Gans, P., and Wemmer, K. (2005). New age constraints on the metamorphic evolution of the high-pressure/low-temperature belt in the Western Tianshan Mountains, NW China. *J. Geol.* 113, 157–168. doi: 10.1086/427666

Klemd, R., Hegner, E., Bergmann, H., Pfander, J. A., Li, J. L., and Hentschel, F. (2014). Eclogitization of transient crust of the Aktyuz Complex during late Palaeozoic plate collisions in the Northern Tianshan of Kyrgyzstan. *Gondwana Res.* 26, 925–941. doi: 10.1016/j.gr.2013.08.018

Konopelko, D., Kullerud, K., Apayarov, F., Sakiev, K., Baruleva, O., Ravna, E., et al. (2012). SHRIMP zircon chronology of HP-UHP rocks of the Makbal metamorphic complex in the Northern Tien Shan, Kyrgyzstan. *Gondwana Res.* 22, 300–309. doi: 10.1016/j.gr.2011.09.002

Kröner, A., Alexeiev, D., Rojas-Agramonte, Y., Hegner, E., Wong, J., Xia, X., et al. (2013). Mesoproterozoic (Grenville-age) terranes in the Kyrgyz North Tianshan: zircon ages and Nd-Hf isotopic constraints on the origin and evolution of basement blocks in the southern Central Asian Orogen. *Gondwana Res.* 23, 272–295. doi: 10.1016/j.gr.2012.05.004

Kröner, A., Alexeiev, D. V., Hegner, E., Rojas-Agramonte, Y., Corsini, M., Chao, Y., et al. (2012). Zircon and muscovite ages, geochemistry, and Nd-Hf isotopes for the Aktyuz metamorphic terrane: evidence for an Early Ordovician collisional belt in the northern Tianshan of Kyrgyzstan. *Gondwana Res.* 21, 901–927. doi: 10.1016/j.gr.2011.05.010

Kröner, A., Kovach, V., Belousova, E., Hegner, E., Armstrong, R., Dolgopolova, A., et al. (2014). Reassessment of continental growth during the accretionary history of the Central Asian Orogenic Belt. *Gondwana Res.* 25, 103–125. doi: 10.1016/j.gr.2012.12.023

Kröner, A., Windley, B. F., Badarch, G., Tomurtogoo, O., Hegner, E., Jahn, B. M., et al. (2007). Accretionary growth and crust-formation in the Central Asian Orogenic Belt and comparison with the Arbian-Nubian shield. *Mem. Geol. Soc. Am.* 200:461. doi: 10.1130/2007.1200(11)

Li, Q.-L., Li, X.-H., Liu, Y., Tang, G.-Q., Yang, J.-H., and Zhu, W.-G. (2010). Precise U-Pb and Pb-Pb dating of Phanerozoic baddeleyite by SIMS with oxygen flooding technique. *J. Analyt. Atom. Spectrom.* 25, 1107–1113. doi: 10.1039/b923444f

Li, X., Tang, G., Gong, B., Yang, Y., Hou, K., Hu, Z., et al. (2013). Qinghu zircon: a working reference for microbeam analysis of U-Pb age and Hf and O isotopes. *Chin. Sci. Bull.* 58, 4647–4654. doi: 10.1007/s11434-013-5932-x

Li, X. H., Liu, Y., Li, Q. L., Guo, C. H., and Chamberlain, K. R. (2009). Precise determination of Phanerozoic zircon Pb/Pb age by multicollector SIMS without external standardization. *Geochem. Geophys. Geosyst.* 10:C002400. doi: 10.1029/2009GC002400

Ludwig, K. R. (2003). Isoplot 3.00: a geochronological toolkit for Microsoft Excel, Berkeley. *Geochronol. Cent. Spec. Publ.* 4:71.

Malyukova, N. (2001). The Taldybulak Levoberezhny gold deposit. Paleozoic geodynamics and gold deposits in the Kyrgyz Tien Shan. *Excurs. Guidebook Ser. Annu. Newsl. IGCP* 373, 97–109.

Orozbaev, R., Takasu, A., Bakirov, A., Tagiri, M., and Sakiev, K. (2010). Metamorphic history of eclogites and country rock gneisses in the Aktyuz area, Northern Tien-Shan, Kyrgyzstan: a record from initiation of subduction through to oceanic closure by continent-continent collision. *J. Metamorph. Geol.* 28, 317–339. doi: 10.1111/j.1525-1314.2010.00865.x

Orozbaev, R. T., Takasu, A., Tagiri, M., Bakirov, A. B., and Sakiev, K. S. (2007). Polymetamorphism of Aktyuz eclogites (northern Kyrgyz Tien-Shan) deduced from inclusions in garnets. *J. Miner. Petrol Sci.* 102, 150–156. doi: 10.2465/jmps.060831b

Ragozin, A. L., Liou, J. G., Shatsky, V. S., and Sobolev, N. V. (2009). The timing of the retrograde partial melting in the Kumdy-Kol region (Kokchetav Massif, Northern Kazakhstan). *Lithos* 109, 274–284. doi: 10.1016/j.lithos.2008.06.017

Rojas-Agramonte, Y., Herwartz, D., García-Casco, A., Kröner, A., Alexeiev, D. V., Klemd, R., et al. (2013). Early Palaeozoic deep subduction of continental crust in the Kyrgyz North Tianshan: evidence from Lu-Hf garnet geochronology and petrology of mafic dikes. *Contribut. Mineral. Petrol.* 166, 525–543. doi: 10.1007/s00410-013-0889-y

Rojas-Agramonte, Y., Kröner, A., Alexeiev, D. V., Jeffreys, T., Khudoley, A. K., Wong, J., et al. (2014). Detrital and igneous zircon ages for supracrustal rocks

of the Kyrgyz Tianshan and palaeogeographic implications. *Gondwana Res.* 26, 957–974. doi: 10.1016/j.gr.2013.09.005

Ryazantsev, A. V., Degtyarev, K. E., Kotov, A. B., Sal'Nikova, E. B., Anisimova, I. V., and Yakovleva, S. Z. (2009). Ophiolite sections of the Dzhalair-Nayman zone, South Kazakhstan: their structure and age substantiation. *Doklady Earth Sci.* 427, 902–906. doi: 10.1134/S1028334X09060038

Seltmann, R., Konopelko, D., Biske, G., Divaev, F., and Sergeev, S. (2011). Hercynian post-collisional magmatism in the context of Paleozoic magmatic evolution of the Tien Shan orogenic belt. *J. Asian Earth Sci.* 42, 821–838. doi: 10.1016/j.jseaes.2010.08.016

Seltmann, R., Porter, T. M., and Pirajno, F. (2014). Geodynamics and metallogeny of the central Eurasian porphyry and related epithermal mineral systems: a review. *J. Asian Earth Sci.* 79(Part B), 810–841. doi: 10.1016/j.jseaes.2013.03.030

Sengor, A. M. C., and Natalin, B. (1994). "Paleotectonics of Asia: fragments of a syn thesis," in *The Tectonic Evolution of Asia*, eds A. Yin and T. M. Harrison (Cambridge: Cambridge University Press), 486–640.

Shatsky, V. S., Jagoutz, E., Sobolev, N. V., Kozmenko, O. A., Parkhomenko, V. S., and Troesch, M. (1999). Geochemistry and age of ultrahigh pressure metamorphic rocks from the Kokchetav massif (Northern Kazakhstan). *Contribut. Mineral. Petrol.* 137, 185–205. doi: 10.1007/s004100050545

Slama, J., Kosler, J., Condon, D. J., Crowley, J. L., Gerdes, A., Hanchar, J. M., et al. (2008). Plesovice zircon - A new natural reference material for U-Pb and Hf isotopic microanalysis. *Chem. Geol.* 249, 1–35. doi: 10.1016/j.chemgeo.2007.11.005

SöDerlund, U., Patchett, P. J., Vervoort, J. D., and Isachsen, C. E. (2004). The 176Lu decay constant determined by Lu-Hf and U-Pb isotope systematics of Precambrian mafic intrusions. *Earth Planet. Sci. Lett.* 219, 311–324. doi: 10.1016/S0012-821X(04)00012-3

Stacey, J. S., and Kramers, J. D. (1975). Approximation of terrestrial lead isotope evolution by a two-stage model. *Earth Planet Sci. Lett.* 26, 207–221. doi: 10.1016/0012-821X(75)90088-6

Tagiri, M., Yano, T., Bakirov, A., Nakajima, T., and Uchiumi, S. (1995). Mineral parageneses and metamorphic P-T paths of ultrahigh-pressure eclogites from Kyrghyzstan Tien-Shan. *ISL Arc.* 4, 280–292. doi: 10.1111/j.1440-1738.1995.tb00150.x

Togonbaeva, A., Takasu, A., Bakirov, A. A., Sakurai, T., and Sakiev, K. (2009). CHIME monazite ages of garnet-chloritoid-talc schists in the Makbal Complex, Northern Kyrgyz Tien-Shan: first report of the age of the UHP metamorphism. *J. Mineral. Petrol. Sci.* 104, 77–81. doi: 10.2465/jmps.081022e

Trifonov, B. (1987). "Ore controlling reverse-thrusting zones in Kyrgyzstan," in *Proceedings of the Conference: Metallogeny of the Tien Shan, Union of Soviet Socialist Repub-lics (USSR)*, Russia, 174–176.

Trifonov, B. (2016). Comment on "Re-Os pyrite and U-Pb zircon geochronology from the Taldybulak Levoberezhny gold deposit: insight for Cambrian metallogeny of the Kyrgyz northern Tien Shan" by Xiaobo Zhao, Chunji Xue, Guoxiang Chi, Nikolay Pak, Bo Zu [Geol. Rev. 67 (2015) 78-89]. *Ore Geol. Rev.* 106, 464–467. doi: 10.1016/j.oregeorev.2016.10.041

Vervoort, J., and Blichert-Toft, J. (1999). Evolution of the depleted mantle: Hf isotope evidence from juvenile rocks through time. *Geochim. Cosmochim. Acta* 63, 533–556. doi: 10.1016/S0016-7037(98)00274-9

Vervoort, J. D., and Patchett, P. J. (1996). Behavior of hafnium and neodymium isotopes in the crust: constraints from Precambrian crustally derived granites. *Geochim. Cosmochim. Acta* 60, 3717–3733. doi: 10.1016/0016-7037(96)00201-3

Wiedenbeck, M., Alle, P., Corfu, F., Griffin, W. L., Meier, M., Oberli, F., et al. (1995). Three natural zircon standards for U-Th-Pb, Lu-Hf, trace element and REE analyses. *Geostand. Newslett.* 19, 1–23. doi: 10.1111/j.1751-908X.1995.tb00147.x

Windley, B. F., Alexeiev, D., Xiao, W., Kröner, A., and Badarch, G. (2007). Tectonic models for accretion of the Central Asian Orogenic Belt. *J. Geol. Soc.* 164, 31–47. doi: 10.1144/0016-76492006-022

Wu, Y., and Zheng, Y. (2004). Genesis of zircon and its constraints on interpretation of U-Pb age. *Chin. Sci. Bull.* 49, 1554–1569. doi: 10.1360/04wd0130

Xi, W., Xia, X. H., Wu, Y. S., Ye, T., and Li, N. (2018). Geological characteristics and ore minerals of the Taldybulak Levoberezhny gold deposit, Kyrgyzstan. *Earth Sci. Front.* 25, 135–150.

Xiao, W., Li, S., Santosh, M., and Jahn, B.-M. (2012). Orogenic belts in Central Asia: correlations and connections. *J. Asian Earth Sci.* 49, 1–6. doi: 10.1016/j.jseaes.2012.03.001

Xiao, W., Windley, B. F., Allen, M. B., and Han, C. (2013). Paleozoic multiple accretionary and collisional tectonics of the Chinese Tianshan orogenic collage. *Gondwana Res.* 23, 1316–1341. doi: 10.1016/j.gr.2012.01.012

Xiao, W. J., Windley, B. F., Yuan, C., Sun, M., Han, C. M., Lin, S. F., et al. (2009). Paleozoic multiple subduction-accretion processes of the southern Altaids. *Am. J. Sci.* 309, 221–270. doi: 10.2475/03.2009.02

Xue, C. J., Zhao, X. B., Mo, X. X., Dong, L. H., Gu, X. X., Nurtaev, B., et al. (2014). Asian gold belt in western Tianshan and its geodynamic setting, metallogenic control and exploration. *Earth Sci. Front.* 21, 128–155.

Yuan, H. L., Gao, S., Dai, M. N., Zong, C. L., Günther, D., Fontaine, G. H., et al. (2008). Simultaneous determinations of U-Pb age, Hf isotopes and trace element compostions of zircon by excimer laser-ablation quadrupole and multiple-collector ICP-MS. *Chem. Geol.* 247, 100–118. doi: 10.1016/j.chemgeo.2007.10.003

Zhang, W., Lentz, D. R., Thorne, K. G., and Massawe, R. J. R. (2020). Late Silurian-Early Devonian slab break-off beneath the Canadian appalachians: insights from the Nashwaak Granite, west-central New Brunswick, Canada. *Lithos* 2020, 358–359. doi: 10.1016/j.lithos.2020.105393

Zhao, X., Xue, C., Chi, G., Chu, H., Li, Z., Pak, N., et al. (2017). Multi-stage gold mineralization in the Taldybulak Levoberezhny deposit, Tien Shan, Kyrgyzstan: reply to comment by Boris Trifonov on "Re-Os pyrite and U-Pb zircon geochronology from the Taldybulak Levoberezhny gold deposit: insight for Cambrian metallogeny of the Kyrgyz northern Tien Shan". *Ore Geol. Rev.* 82, 217–231. doi: 10.1016/j.oregeorev.2016.10.042

Zhao, X., Xue, C., Chi, G., Pak, N., and Zu, B. (2015). Re-Os pyrite and U-Pb zircon geochronology from the Taldybulak Levoberezhny gold deposit: insight for Cambrian metallogeny of the Kyrgyz northern Tien Shan. *Ore Geol. Rev.* 67, 78–89. doi: 10.1016/j.oregeorev.2014.12.002

Zhimulev, F. I., Buslov, M. M., Travin, A. V., Dmitrieva, N. V., and De Grave, J. (2011). Early-Middle Ordovician nappe tectonics of the junction between the Kokchetav HP-UHP metamorphic belt and the Stepnyak paleoisland arc (northern Kazakhstan). *Russian Geol. Geophys.* 51, 190–203. doi: 10.1016/j.rgg.2010.12.009

Zhou, G., Liu, H., Chen, K., Gai, X., Zhao, C., Liao, L., et al. (2018). The origin of pyroelectricity in tourmaline at varying temperature. *J. Alloys Compounds* 744, 328–336. doi: 10.1016/j.jallcom.2018.02.064

Zhou, L., McKenna, C. A., Long, D. G. F., and Kamber, B. S. (2017). LA-ICP-MS elemental mapping of pyrite: an application to the Palaeoproterozoic atmosphere. *Precambr. Res.* 297, 33–55. doi: 10.1016/j.precamres.2017.05.008

Zhu, Y., He, G. Q., and An, F. (2007). Geological evolution and metallogeny in the core par t of the central Asian metallogenic domain. *Geol. Bull. China* 26, 1167–1177.

Conflict of Interest: XX was employed by Sichuan Geological and Mineral Resources Group Co., Ltd. and by Altynken Limited Liability Company, Zijin Mining Group.

The remaining authors declare that the research was conducted in the absence of any commercial or financial relationships that could be construed as a potential conflict of interest.